PHYSICAL REVIEW B VOLUME 45, NUMBER 7 15 FEBRUARY 1992-I

Properties of thin strained layers of GaAs grown on InP

M.-E. Pistol, M. Gerling, D. Hessman, and L. Samuelson
Department of Solid State Physics, University of Lund, Box 118, S-221 00 Lund, Sweden
(Received 21 June 1991)

Single strained layers of GaAs grown on InP have been studied by a variety of optical experiments. Raman spectroscopy shows the strain-shifted LO^{Γ} phonon, thus proving that the layers are strained. The photoluminescence is strong, allowing photoluminescence excitation spectroscopy to be performed in a diamond-anvil cell. The absorption is found to increase slowly close to the threshold. A theory of absorption in type-II quantum wells is used in order to compare with experiment. Photoconductivity and modulated-reflectance experiments have been carried out on the samples and indications of the presence of heavy-hole states are seen. The strain Hamiltonian of the valence band has been transformed into a 6×6 matrix, which is parametrized by the strain-tensor elements, allowing easy calculation of the strain shift of the band edges even in unusual strain situations. The experimental results are consistent with a marginally type-II structure in which the holes are confined to the GaAs layer but the electrons reside in the InP layers.

I. INTRODUCTION

With the development of modern growth techniques such as metal-organic vapor phase epitaxy[1] (MOVPE) and molecular-beam epitaxy,[2] it has become possible to grow perfect epitaxial structures containing semiconductor layers with unequal lattice constants. Such structures then contain layers with elastically strained crystal lattices. This strain will affect the band structure of the material, allowing the fabrication of materials in which the band gap and the lattice constant are independently variable, although within limits.[3] The ability to fabricate such "strained" epitaxial layers thus offers extra flexibility in materials science. If the strained layer is very thin (<200 Å) a quantum well will be formed and quantum size effects will be seen. The quantum well may be type I, which is the best known case, in which a well is formed for both electrons and holes.[4] In some cases a type-II quantum well will form in which the strained layer forms a well for one of the charge carriers and a barrier for the other type of charge carrier.[5] The absorption and recombination cross sections in a type-II quantum well are believed to be much reduced in comparison with a type-I quantum well,[6] although we will argue that the absorption is higher than is usually believed for thin type-II quantum wells, where the electron-hole overlap might be large. Recombination of charge carriers occurs across the interfaces of the layer and is strongly affected by impurities at the interface.[7] An interesting system is $Ga_xIn_{1-x}As$ strained to InP which can exhibit both type-II and type-I behavior, where $Ga_xIn_{1-x}As$ strained to InP is type I for $x<0.8$ but is a type-II system for $x>0.8$ as established by Gershoni *et al.*[8] However no detailed optical study was done in Ref. 8.

In this paper we first describe the growth, by reduced pressure MOVPE, of thin strained layers of GaAs in between InP. In Sec. III we present a summary of deformation potential theory and give the general strain Hamiltonian in a matrix form. In Sec. IV we describe the experiments (photoluminescence, photoluminescence excitation spectroscopy, photoconductivity, electroreflectance, and Raman spectroscopy, some of which have been performed under hydrostatic pressure), and compare them with theoretical predictions. Finally in Sec. V we give some conclusions.

II. GROWTH AND EXPERIMENT

Double heterostructures of InP/GaAs/InP were grown by MOVPE on (001)-oriented, Sn-doped InP substrates, at a pressure of 50 mbar. The horizontal reactor cell had a rectangular cross section. The growth system was designed for rapid gas switching having a compact ventrun manifold with a pressure balance of better than 0.1 mbar. A growth temperature of 600 °C was used. As starting compounds, trimethyl gallium (TMGa), trimethyl indium (TMIn), phosphine (PH_3), and arsine (AsH_3) were used with Pd-purified hydrogen as the carrier gas. The total flow rate was about 5860 cm^3/min.

During the heat-up state PH_3 was used to protect the substrate surface. Upon reaching the growth temperature, we started with the deposition of about 2.5 μm InP as a buffer layer, followed by a thin GaAs layer, and finally a cladding layer of about 250 Å of InP. The transition between barrier and quantum well was performed by a 2-s growth interrupt: switching off the TMIn at the beginning of this step, switching off the PH_3 and on the AsH_3 one second later, and finally switching on TMGa after one more second to start the growth of the quantum well. The inverse procedure was used upon the completion of the quantum well. Two samples were grown, having estimated GaAs thicknesses of 18 Å and 28 Å. The actual thicknesses are not known with certainty since no transmission electron microscopy has been performed on the samples. Low-temperature spectrally resolved cathodoluminescence showed that the samples were totally

 ©1992 The American Physical Society

strained and that no misfit dislocations of the 60° type were present at the interfaces.[9] Calculations of the critical thickness, according to the theory of Matthews and Blakeslee[10] give a value of about 30 Å, assuming that misfit dislocations of the 60° type are formed at both interfaces. This calculated critical thickness is in agreement with our cathodoluminescence results. Gershoni *et al.*[8] found a critical thickness of about 16 Å, which is the critical thickness obtained if one assumes that the misfit dislocations are formed at only one interface. The experimental difference might be due to the different growth techniques used (gas-source molecular beam epitaxy in Ref. 8 versus metal-organic vapor phase epitaxy in our case). In particular, the growth rate must be so high that the strained layer does not have enough time to relax before the capping layer has started to form in order to obtain a higher value for the critical thickness.

For the photoluminescence and Raman measurements the 5145-Å (for PL) or the 4880-Å (for Raman) line from Ar^+ were used with a typical excitation power of 20 mW. A sapphire:Ti tunable laser, stabilized to give a constant laser power, was used for the PLE measurements. The emission was focused on the entrance slit of a double monochromator and detected with a photomultiplier. A CCD camera cooled with liquid nitrogen was used to detect Raman scattered light, with a typical integration time of 5 min. The samples were polished to a thickness of about 30 μm, broken into small pieces, and loaded into a diamond-anvil cell, Merril-Bassett type, using Ar as the pressure transmitting medium, in order to do the hydrostatic pressure measurements. For the electro-optical experiments a thin (75 Å) transparent layer of Au was evaporated of the surface of the crystal to make a Schottky contact and Sn, Au, and Cr were alloyed to the back of the crystal to make an Ohmic contact. A halogen lamp and the monochromator were used for the reflectance measurements with a germanium diode to detect the reflected light.

III. DEFORMATION-POTENTIAL THEORY

The built-in strain in thin layers of semiconductors grown pseudomorphically on substrates with a different lattice constant shifts the energy positions of the valence- and conduction-band edges. The shift of the band edges can be calculated via linear deformation-potential theory for small values of the strain, such as those occuring in this work. The strain Hamiltonian for the valence band can be written as[11]

$$H=H_1+H_2\ , \tag{1}$$

where H_1 contains the orbital strain terms and can thus be written as

$$\begin{aligned}H_1=&-a_1(e_{xx}+e_{yy}+e_{zz})-3b_1[(L_x^2-\tfrac{1}{3}\mathbf{L}^2)e_{xx}+\text{c.p.}]\\&-\sqrt{3}d_1[(L_xL_y+L_yL_x)e_{xy}+\text{c.p.}]\end{aligned} \tag{2}$$

and H_2 contains the strain-dependent spin-orbit terms, as follows:

$$\begin{aligned}H_2=&-a_2(e_{xx}+e_{yy}+e_{zz})\mathbf{L}\cdot\boldsymbol{\sigma}\\&-3b_2[(L_x\sigma_x-\tfrac{1}{3}\mathbf{L}\cdot\boldsymbol{\sigma})e_{xx}+\text{c.p.}]\\&-\sqrt{3}d_2[(L_x\sigma_y+L_y\sigma_x)e_{xy}+\text{c.p.}]\ .\end{aligned} \tag{3}$$

Here $\mathbf{L}$ and $\boldsymbol{\sigma}$ are the angular-momentum operator and the Pauli spin matrix, respectively. The parameters a_1, a_2, b_1, b_2, d_1, and d_2, are the experimentally determined deformation potentials. The strain-tensor components are present as the parameters e_{ij}. The strain Hamiltonian H_Γ, for the Γ conduction band has the eigenvalue[11]

$$C_1(e_{xx}+e_{yy}+e_{zz})\ . \tag{4}$$

The strain Hamiltonian for the X conduction band H_X has the following eigenvalues in our strain situation [growth on the (001) surface]:[11]

$$E_1(e_{xx}+e_{yy}+e_{zz})+\tfrac{2}{3}E_2(e_{zz}-e_{xx})\ , \tag{5a}$$

$$E_1(e_{xx}+e_{yy}+e_{zz})-\tfrac{1}{3}E_2(e_{zz}-e_{xx})\ , \tag{5b}$$

where C_1, E_1, and E_2 are deformation potentials, and the growth axis is taken along the z direction. The eigenvalue given by Eq. (5a) is for the X valley along the growth direction, while the eigenvalue given by Eq. (5b) is for the X valley perpendicular to the growth direction. In order to find the energy levels under strain, i.e., given a particular set of e_{ij}, it is necessary to find the eigenvalues of the relevant conduction-hand Hamiltonians H_Γ and H_X and then the eigenvalues of the valence-band Hamiltonian H_1+H_2. Since there is an increasing interest in growing strained layers on unusual crystal planes we will give the full valence-hand Hamiltonian in a matrix form parametrized by the deformation potentials and the strain-tensor elements for future reference. We first transform the valence-band Hamiltonian H_1+H_2 to a Hamiltonian matrix, which we call $\underline{M}$. Defining $\text{Tr}e=e_{xx}+e_{yy}+e_{zz}$ and $E_\theta=2e_{zz}-e_{yy}-e_{xx}$, we get

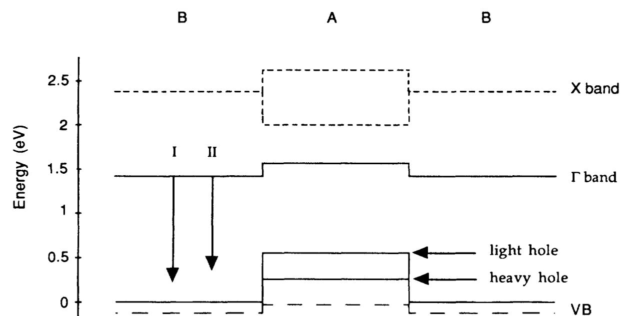

FIG. 1. A potential energy diagram of strained GaAs grown on InP. The GaAs layer is denoted by A and the InP layers by B. The light- and heavy-hole band edges of the GaAs layer are indicated. The spin-orbit split-off band is represented by the dashed line in the valence band. The transition energies are indicated by vertical arrows (I for the heavy hole and II for the light hole) assuming a GaAs layer width of 28 Å.

TABLE I. Constants for GaAs used in the calculation of the potential energy diagram shown in Fig. 1. The values are taken from the Landolt-Börnstein tables (Ref. 14) unless noted. These revised values are used in order to fit published hydrostatic pressure measurements.

S_{11}	S_{12}	$C_1+a_1+a_2$	$C_1+a_1-2a_2$	b_1	b_2	$E_1+a_1+a_2$	E_2
1.163 Mbar^{-1}	-0.370 Mbar^{-1}	-8.5 eV[a]	-8.5 eV[b]	-1.7 eV	0 eV	1.06 eV[a]	8.6 eV[c]

[a]From Ref. 15.

[b]This value is not known to the authors and was set equal to $C_1+a_1+a_2$. This implies that the spin-orbit splitting is independent of hydrostatic pressure.

[c]From Ref. 16.

$$\underline{M}=\begin{bmatrix} X_1 & 0 & X_4^* & O_1^* & X_5^* & O_2^* \\ 0 & X_1 & O_1 & -X_4 & -O_2 & X_5 \\ X_4 & O_1^* & X_2 & 0 & X_6^* & O_3^* \\ O_1 & -X_4^* & 0 & X_2 & O_3 & -X_6 \\ X_5 & -O_2^* & X_6 & O_3^* & X_3 & 0 \\ O_2 & X_5^* & O_3 & -X_6^* & 0 & X_3 \end{bmatrix}, \quad (6)$$

where we are using the basis functions $|\frac{3}{2},\frac{3}{2}\rangle$, $|\frac{3}{2},-\frac{3}{2}\rangle$, $|\frac{3}{2},\frac{1}{2}\rangle$, $|\frac{3}{2},-\frac{1}{2}\rangle$, $|\frac{1}{2},\frac{1}{2}\rangle$, and $|\frac{1}{2},-\frac{1}{2}\rangle$, which also label the rows and the columns of the matrix in this order, starting from the top left corner. The first quantum number is the total angular momentum J and the second is the projection J_z along the z direction. A superscript asterisk indicates complex conjugation. The matrix elements are[12]

$$\begin{aligned} X_1&=-(a_1+a_2)\mathrm{Tr}e-\tfrac{1}{2}(b_1+2b_2)E_\theta\ ,\\ X_2&=-(a_1+a_2)\mathrm{Tr}e+\tfrac{1}{2}(b_1+2b_2)E_\theta\ ,\\ X_3&=-(a_1-2a_2)\mathrm{Tr}e-\Delta_0\ ,\\ X_4&=-(d_1+2d_2)(ie_{yz}+e_{zx})\ ,\\ X_5&=(\sqrt{2}/2)(d_1-d_2)(ie_{yz}+e_{zx})\ ,\\ X_6&=-(\sqrt{2}/2)(b_1-b_2)E_\theta\ ,\\ O_1&=\sqrt{3}\left[\frac{b_1}{2}+b_2\right](-e_{xx}+e_{yy})-i(d_1+2d_2)e_{xy}\ ,\\ O_2&=\sqrt{3/2}(b_1-b_2)(e_{xx}-e_{yy})+i\sqrt{2}(d_1-d_2)e_{xy}\\ O_3&=-\sqrt{3/2}(d_1-d_2)(ie_{yz}+e_{xz})\ . \end{aligned} \quad (7)$$

Here Δ_0 is the spin-orbit splitting in the valence band and i is the imaginary unit. By using the eigenvalues given in Eq. (4) or (5) (with the unstrained band gap added) and the eigenvalues of the matrix $\underline{M}$ defined in Eq. (6) one obtains the relevant energy levels. It is necessary that the deformation potentials are known (or can be educatedly guessed), which is not always the case. If only the sum $C_1+a_1+a_2$, (or $E_1+a_1+a_2$) is experimentally known, which is often the case, the same energy levels will be obtained if C_1 is replaced by $C_1+a_1+a_2$ in Eq. (4) [or E_1 with $E_1+a_1+a_2$ in Eqs. (5a) and (5b)], followed by a diagonalization of the matrix M, however with the terms involving a_1 and a_2 removed. This implies that $a_2=0$, which is usually a good approximation. Note that the above treatment is quite general and can easily be applied to growth on unusual crystal planes as well as to applied uniaxial strain and hydrostatic pressure, as long as the strain-tensor elements are known.[13] Great care should be taken when using experimentally obtained values of the deformation potentials d_1 and d_2, since there are two conventions in the definitions of the off-diagonal strain-tensor elements differing by a factor of 2.[13]

The finite strain-tensor elements for a strained layer grown on the (001) surface are

$$e_{zz}=2\frac{S_{12}}{S_{12}+S_{11}}e_{xx},\quad e_{xx}=e_{yy}=-f\ , \quad (8)$$

where S_{11} and S_{12} are the elastic compliances and f is the misfit, which is defined as $f=(a_{\text{layer}}-a_{\text{substrate}})/a_{\text{layer}}$, where a_i are the unstrained lattice constants. For a material grown in tension such as GaAs grown on InP, $e_{xx}>0$.

Using the constants given in Table I we have performed a calculation of the energy structure of GaAs strained to InP at atmospheric pressure using the theory developed above. The unstrained valence-band offset was chosen to be 0.38 eV in order to fit the data given in Ref. 8. A potential diagram of the result is shown in Fig. 1. A marginally type-II structure is found. The potential step in the conduction band is very small, about 130 meV, which must be remembered when interpreting some of the experiments. This conduction-band step is a sensitive function of the parameters, especially the valence-band offset. The lowest state in the strained valence band, ignoring quantum size effects, is the light-hole band with the heavy-hole state being about 310 meV higher in energy (for holes). The X band in the strained GaAs layer is strongly split with an energy difference of about 630 meV between the X_z and the X_{xy} states (with X_z, which has a wave vector parallel to the growth direction, being lowest in energy). Wang and Stringfellow found that InP/GaAs/InP should be marginally type I.[17] The difference is easily explained by the sensitivity of the result to the choice of the unstrained valence-band offset. Wang and Stringfellow used data where the unstrained valence-band offset is a function of hydrostatic pressure. Recent data, however, show that the valence-band offset is not a function of hydrostatic pressure.[18,19]

IV. EXPERIMENTAL RESULTS

A. Photoluminescence and photoluminescence excitation spectroscopy

Figure 2 shows the low-temperature photoluminescence (PL) spectra of the two samples, having GaAs thicknesses of 18 Å and 28 Å, and an insert of the energy structure along with the recombination path. It can be seen that the emission consists of several peaks and that there is a quantum size effect. The emission is concluded not to be due to deep levels in the InP barrier. A simple effective mass calculation[6,20] has been performed to calculate the energy levels and gives transition energies of 1.08 and 1.19 eV. A light-hole mass of $0.07m_0$ was used. The agreement with experiment is satisfactory. We will, in the rest of this section and in Sec. V, provide arguments that the emission we observe is indeed close to the band-to-band transition energy.

In order to determine the nature of the peaks we performed PL at different spots on the wafer. If the different peaks are due to monolayer fluctuations within the layer, their intensity, but not their position, should be a strong function of the spatial position on the wafer, as has been established from studies of Ga-In-As quantum wells in InP grown in the same machine under similar growth conditions.[21] There are no strong intensity variations of the peaks across the wafer in the sample with the 18-Å GaAs well, but a rather small shift of the position of the peaks. Intensity measurements, shown in Fig. 3, show that the low-energy peak in the 18-Å sample have a sublinear dependence on the excitation power density. This is also true for the high-energy peak. This implies that we are most likely not seeing exciton recombination in these type-II quantum wells, but rather PL from interface defects (however where one of the charge carriers, most likely the hole, is experiencing quantum size effects). It is of considerable interest to know how close in energy the observed emission is to the emission energy expected from a cross interface recombination as indicated in Fig. 2. We have performed photoluminescence excitation (PLE) spectroscopy on the samples, while monitoring the layer emission. PLE is closely related to absorption and should be a more appropriate tool than PL to determine the energy of a band-to-band transition. This experiment had to be performed in a diamond-anvil cell, opening up the energy gap to a suitable value for our tunable laser. Detailed hydrostatic pressure experiments on this material system have been published elsewhere.[18,19] The spectra are displayed in Figs. 4, 5, and 6. It was impossible to cover the whole energy range between the emission and the InP band gap in the thicker sample in one measure-

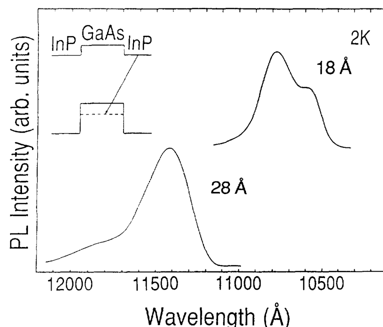

FIG. 2. The photoluminescence spectra of strained GaAs grown on InP. The upper curve is the spectrum of the sample with the 18-Å GaAs well and the lower curve is the spectrum of the sample with the 28-Å GaAs well.

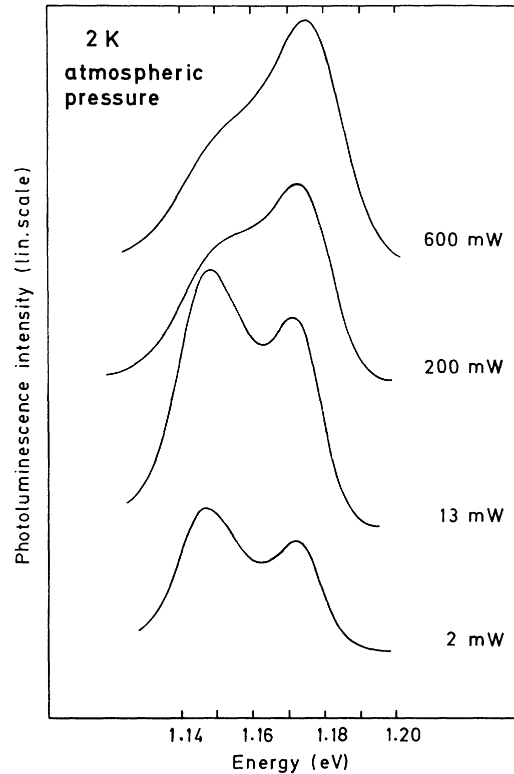

FIG. 3. The photoluminescence spectrum of the 18-Å sample at different excitation powers.

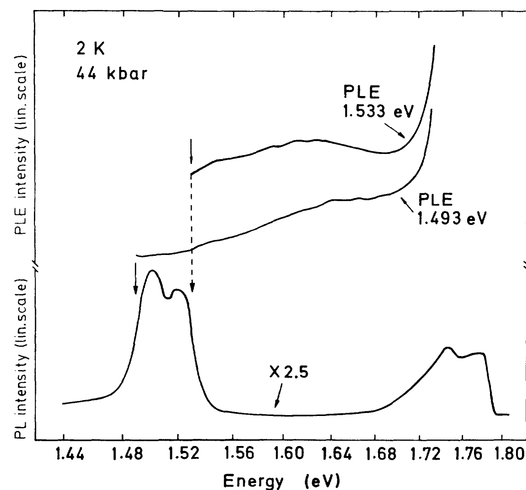

FIG. 4. The photoluminescence excitation spectra of the 18-Å sample at a pressure of 44 kbar, along with the photoluminescence spectrum.

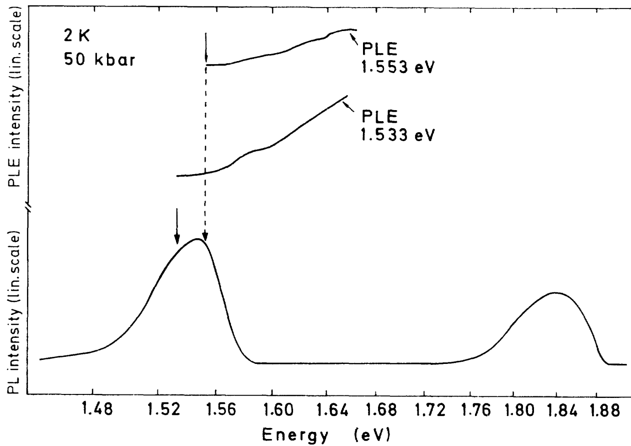

FIG. 5. The photoluminescence excitation spectra of the 28-Å sample close to the emission, along with the photoluminescence spectrum. The spectra were taken at a pressure of 50 kbar.

ment. Close to the emission energy there is an increase in the signal which soon levels off, which is clearly seen in the 18-Å sample; see Fig. 4. There is some structure at an energy of about 100 meV higher than the emission energy in this sample. At higher energy there is a strong increase in the signal at the InP band gap for both samples. Detection at different emission energies gives almost the same excitation spectra. The small differences that are seen are most likely due to insufficient stabilization of the laser. We conclude that the high-energy PL emission is close in energy to that expected from a band-to-band transition.

Bastard has calculated the absorption in a type-II quantum well[6] and predicts an increase, proportional to $(E-E_0)^{3/2}$ in the absorption close to the threshold E_0. At higher energies the absorption becomes constant. The electrons in the surrounding material, InP in our case, do not penetrate the layer barrier in this calculation, i.e., the GaAs barrier for electrons is assumed to be infinitely high. In our case where the barrier for electron is quite low we believe that it is necessary to take into account the penetration of the electron wave function into the layer. We will use a refinement of Bastard's theory in the next section, where this is taken into account.

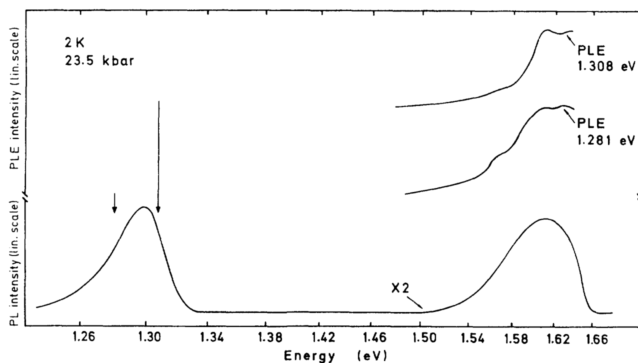

FIG. 6. The photoluminescence excitation spectra of the 28-Å sample close to the InP emission, with the detection energy indicated by arrows, along with the photoluminescence spectrum. These spectra were taken at a pressure of 23.5 kbar.

B. Photoconductivity and electroreflectance

Figure 7 shows the PL, photoconductivity (PC), and electroreflectance (ER) spectra of the 28-Å sample, while Fig. 8 shows the same type of spectra for the 18-Å sample. These experiments have been performed at atmospheric pressure. The PC spectra are similar to the PLE spectra, cf. Fig. 4, and show that the PL emission is close to the energy expected from a band-to-band transition also at atmospheric pressure. Close to the threshold there is an increase in the signal which soon levels off, this being especially clear in the 28-Å sample. The 28-Å sample shows very clearly the thermalization to the interface states that have an emission energy which is about 10 meV lower than the onset of the PC signal. There are indications of excited states around 1.3 eV in both samples as seen in both PC and ER, and this is similar to what was seen in PLE. Calculations using the effective mass theory give transition energies of 1.08 eV for the light hole and 1.22 eV for the heavy hole in the 28-Å sample. For the 18-Å sample the corresponding energies are 1.19 eV for the light hole and 1.25 eV for the heavy hole. There are no further bound-hole states, according to this theory. It is predicted from theory that peaks in absorption and electroreflectance overestimate transition energies. It is also seen in PLE and PC spectra that the onset of absorption is gentle. We attribute the peaks around 1.3 eV, in both samples, to transitions between the heavy hole in the valence band of the strained layer and the conduction-band minimum in InP.

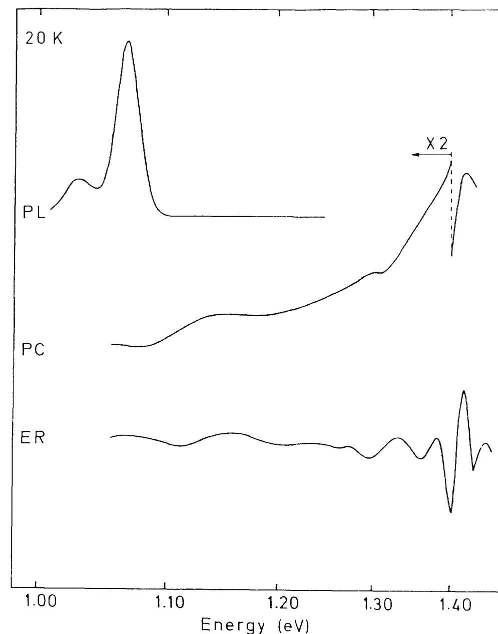

FIG. 7. The photoluminescence (PL), photoconductivity (PC), and the electroreflectance (ER) spectra of the 28-Å sample.

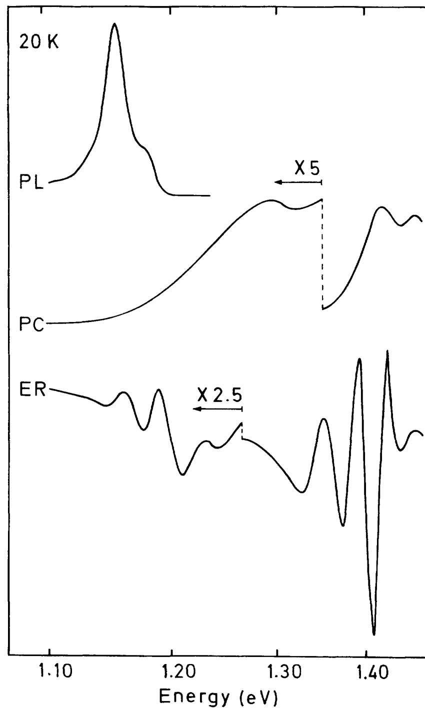

FIG. 8. The photoluminescence (PL), photoconductivity (PC), and the electroreflectance (ER) spectra of the 18-Å sample.

We have calculated the absorption in a type-II quantum well using a simple model, which is aimed at some qualitative understanding. If we denote the GaAs layer with A and the InP layers with B, see Fig. 1, it is possible to solve the Schrödinger equation in regions A and B, as is done in the envelope-function approximation, where constant potentials are used in each region.[20] Due to the low barrier for electrons we account for the penetration of the electron wave function into the barrier. Following Bastard, the absorption is given as the square of the overlap of the electron and hole wave functions, integrated over the allowed transitions. Figure 9(a) shows the result both for this model and for Bastard's model[6] using a well width of 28 Å and different barrier heights for the electrons. The curve with a barrier height of 140 meV corresponds to the sample with a GaAs thickness of 28 Å. There is initially an increase in the absorption which soon levels off to an almost constant value. The rate of increase is slower for a well with a higher barrier. The absorption is stronger in our model than in Bastard's model. This is reasonable, since the electron-hole overlap is very strong when the electron energy is above the barrier and the electron wave function fully penetrates the strained layer. It is clear from the PLE and PC experiments that, experimentally, the absorption increase is faster, and the plateau is more pronounced than theory predicts, given our estimated barrier height of 140 meV. We speculate that excitonic effects are at play, where excitons involving electrons in conduction-band minimum in the InP layer and excitons involving electrons in the conduction-band minimum in the GaAs layer should be accounted for. Figure 9(b) illustrates the effect of changing the well width using a constant barrier height of 140 meV. The absorption becomes more steplike for wider wells when the amplitude of the electron wave function becomes small inside the well. It is possible to use this model also when the barrier for electrons is zero, which is illustrated in Fig. 9(a). It is seen that the absorption lineshape has a gentle onset but is beginning to resemble the type-I case in which the onset is a step (ignoring excitonic effects).[6]

The theory of electroreflectance spectra in three dimensions has been treated by Aspnes, and a complicated line shape is found.[22] Klipstein and Apsley have computed the expected ER spectra in type-I quantum wells and compared them with experiments.[23] It was found that the peaks in ER closely correspond to peaks in PL and PLE. If the absorption is known with and without electric field it is possible to do a Kramers-Kronig transformation of the imaginary part of the dielectric function and get the full complex refractive index as a function of electric field which in turn will allow the ER spectrum to be computed. Interference effects have also to be accounted for.[23,24] We have unfortunately not been able to see any changes in the PC spectra with electric field so we

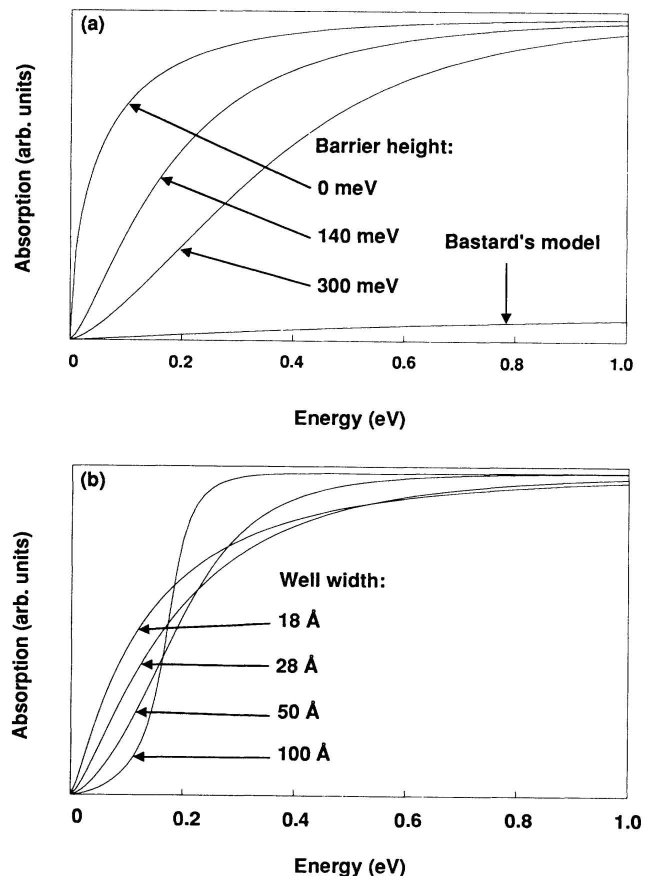

FIG. 9. The calculated absorption spectra. (a) The effect of changing the barrier height for electrons is displayed along with Bastard's model which corresponds to an infinite barrier height. The well width is 28 Å. (b) The effect of changing the well width is displayed. The barrier height is 140 meV.

could not do this comparison. However with the assumption that the electric field will only shift the absorption in energy we have done a calculation, for the 28-Å sample, which reproduces the gross features of the ER spectrum, close to the absorption edge. These calculations show agreement between experiment, show in Fig. 7, and theory with regard to line-width and position of the ER spectrum. The theoretical lineshape did not agree with experiment, unless we calculated the interference using a top InP layer of 350 Å instead of the actual thickness of 250 Å. It can be seen from Figs. 7 and 8 that the ER signal occurs at a higher energy than the PL emission, in contrast to the situation in a type-I quantum well.

C. Raman spectroscopy

Raman spectroscopy gives information on the phonons in strained layers as well as on the crystal quality.[25] Although a substantial amount of work has been done on superlattices, there has not been much work done on single strained layers. This is probably due to the low light levels available, which however can be efficiently overcome by the use of a cooled CCD camera. Figure 10 shows the Raman spectra of the two samples and two reference samples (InP and GaAs). The spectra were taken in the backscattering configuration from the (001) face of the crystals at room temperature. The polarization of the incident light was parallel to the [100] direction while the polarization of the scattered light was parallel to the [010] direction. The LO^{Γ} phonon from InP is a prominent feature, as expected in this scattering geometry. Scattering from the TO^{Γ} phonon is forbidden and can only be seen through crystal imperfections.[26] We see only weak TO^{Γ} scattering with a Raman shift of about 300 cm^{-1} indicating an excellent quality of the samples. In the two-phonon region with a Raman shift of about 260 cm^{-1} there is an extra peak in the strained-layer samples with a Raman shift of about 268 cm^{-1}. This peak is strongest in the 28-Å sample but can be seen as a shoulder in the 18-Å sample. We attribute this peak to a strain-shifted LO^{Γ} phonon in the GaAs layer. This was confirmed by using a scattering geometry where both the incident light and the scattered light were polarized parallel to [010]. In this case a strong reduction of the LO^{Γ} peaks was seen including the strain-shifted LO^{Γ} mode. A Raman spectrum of GaAs is included in the figure for comparison. The LO^{Γ} phonon splits, in strained layers, into a singlet with vibration along the [001] direction, perpendicular to the crystal surface and a doublet with vibration parallel to the (001) surface.[25,27] Only LO^{Γ} phonons with a **k** vector perpendicular to the (001) surface can be seen in backscattering, i.e., the singlet. For this phonon we get a strain shift of[25,27]

$$\frac{\Delta\omega}{\omega_0} = \frac{K_{11}}{2} e_{zz} + \frac{K_{12}}{2} (e_{xx} + e_{yy}) , \quad (9)$$

while for the doublet

$$\frac{\Delta\omega}{\omega_0} = \frac{K_{11}}{2} e_{xx} + \frac{K_{12}}{2} (e_{yy} + e_{zz}) . \quad (10)$$

The frequency shift of the phonon is given by $\Delta\omega$ and the unstrained frequency by ω_0. The deformation potentials $K_{11} = -2$ and $K_{12} = -2.7$ are known from Raman studies of GaAs under uniaxial stress.[28] The strain-tensor elements are designated e_{xx}, e_{yy}, and e_{zz}. The calculated position of the strain-shifted LO^{Γ} phonon replicas, singlet and doublet, are indicated by arrows in Fig. 6 and the shift of the singlet is found to agree within 10% of the experimental value. We thus conclude that the GaAs layers are strained.

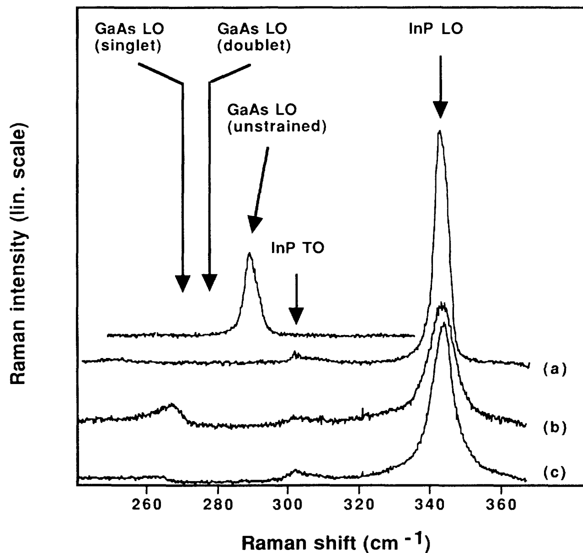

FIG. 10. The Raman spectra of the strained layers. Included are two reference spectra from InP and GaAs. Curve (*a*) is the spectrum of InP for reference. Curve (*b*) is the spectrum of the 28-Å sample, while curve (*c*) is the spectrum from the 18-Å sample. The top curve is the spectrum from GaAs.

V. SUMMARY AND DISCUSSION

We have investigated strained layers of GaAs in InP grown by reduced pressure MOVPE, having excellent optical quality. The possibility to grow highly strained systems of binary-compound semiconductors is of great importance, since alloys may be simulated by short-period binary-compound superlattices, thus alleviating the problems of alloy composition and homogeneity. The photoluminescence from this system is stronger than the InP band-gap emission, allowing photoluminescence excitation spectroscopy to be performed on the samples in a diamond-anvil cell. By using Raman spectroscopy we have seen the strain-shifted LO^{Γ} phonon of GaAs thus proving that the samples were strained. The strain shift of the LO^{Γ} phonon agrees well with theory. This type of structure is believed to be a type-II quantum well from polarized photocurrent spectroscopy, although theoretical calculations show that it is only marginally type II, using established values for deformation potentials and the valence-band offset. Small changes in these values will easily produce a type-I quantum well (theoretically). It is actually very hard to prove that a structure is type II

instead of a type-I structure in which there is a very small confinement for one of the charge carriers (electrons in this case). Using the envelope-function approximation to calculate the energies of the photoluminescence peaks gives good agreement with experiments for our samples. Absorption in a type-II quantum well is qualitatively different from absorption in a type-I quantum well and could be a tool to establish whether a sample is type II or type I. We have performed photoluminescence excitation spectroscopy and photocurrent spectroscopy on our samples. Although these experiments are not directly measuring absorption they should give some information about the transition probabilities as a function of energy. A theory of absorption in type-II structures was used to compare with the experiments. The theory predicts a quite high absorption and a gentle increase in the absorption close to the threshold followed by a region of almost constant absorption. This agrees qualitatively with our experiments. The difference might easily be due to effects neglected in the theory, such as warping of the bands and excitons. By changing the valence-band offset and calculating the absorption in a structure which is in between type II and type I, with no potential step for the electrons, we find that the absorption has a similar shape to the lineshape in a type-II quantum well. It is thus difficult to draw definite conclusions from absorption measurements. It is believed that the photoluminescence in a type-II quantum well is very sensitive to an electric field in contrast to the type-I case. But this is not true if one of the charge carriers is weakly bound in the type-I well, where a pronounced sensitivity to electric fields should be presented. In addition if the photoluminescence from the type-II quantum well is due to interface defects there might be a reduction in the sensitivity to electric fields. We have measured the photoluminescence under electric fields but the results were not conclusive. Only some of the peaks quenched rapidly. Electroreflectance was also performed on the samples. The electroreflectance spectra were quite broad and situated at a higher energy than the photoluminescence peaks, in contrast to the situation in strongly type-I quantum wells. A qualitative agreement with theory based on a Kramers-Kronig transform was found.

Our experiments support the conclusion of Gershoni *et al.*[8] that GaAs strained to InP is type II.

ACKNOWLEDGMENTS

We gratefully acknowledge the helpful support in the growth of the samples by W. Seifert, J.-O. Fornell, and L.-Å. Ledebo at Epiquip AB. We thank G. Grossman for verifying some of the calculations. This work, which was performed within the nm-structure consortium in Lund, was supported by the Swedish Natural Science Research Council and the Swedish National Board for Technical Development.

[1]A. Y. Cho, Appl. Phys. Lett. **19**, 467 (1971).
[2]M. J. Ludowise, J. Appl. Phys. **58**, R31 (1985).
[3]G. C. Osbourn, J. Vac. Sci. Technol. B **1**, 379 (1983).
[4]P. M. Frijlink and J. Maluenda, Jpn. J. Appl. Phys. **21**, L574 (1984).
[5]G. Danan, B. Etienne, R. Mollot, R. Planel, A. M. Jean-Louis, F. Alexandre, B. Jusserand, G. Le Roux, J. Y. Marzin, H. Savary, and B. Sermage, Phys. Rev. B **35**, 6207 (1987).
[6]G. Bastard, *Wave Mechanics Applied to Semiconductor Heterostructures* (Les Editions de Physique, Paris, 1988).
[7]B. A. Wilson, IEEE J. Quantum Electron. **24**, 1763 (1988).
[8]D. Gershoni, H. Temkin, J. M. Vandenberg, S. N. G. Chu, R. A. Hamm, and M. B. Panish, Phys. Rev. Lett. **60**, 448 (1988).
[9]M.-E. Pistol, A. Gustafson, M. Gerling, L. Samuelson, and H. Titze, J. Cryst. Growth **107**, 458 (1991).
[10]J. W. Matthews and A. E. Blakeslee, J. Cryst. Growth **27**, 118 (1974).
[11]L. D. Laude, F. H. Pollak, and M. Cardona, Phys. Rev. B **3**, 2623 (1971).
[12]The matrix elements were computed using a symbolic-algebra computer program. Two different programs using two different methods were written in order to verify the correctness of the calculation.
[13]A lucid treatment of strain tensors in different coordinate systems is given in J. C. Hensel and G. Feher, Phys. Rev. **129**, B1041 (1963), Appendix A.
[14]*Physics of Group-IV Elements and III-V Compounds,* edited by O. Madelung, Landolt-Börnstein, Vol. 17a (Springer-Verlag, Heidelberg, 1982).
[15]D. J. Wolford and J. A. Bradley, Solid State Commun. **53**, 1069 (1985).
[16]Chris G. van de Walle, Phys. Rev. B **39**, 1871 (1989).
[17]T. Y. Wang and G. B. Stringfellow, J. Appl. Phys. **67**, 345 (1990).
[18]M.-E. Pistol, M. Gerling, L. Samuelson, W. Seifert, J.-O. Fornell, and L.-Å Ledebo, in *Proceedings of the 20th International Conference on the Physics of Semiconductors, Thessaloniki, 1990,* edited by E. M. Anastassakis and J. D. Joannopoulos (World Scientific, Singapore, 1990), p. 973.
[19]M. Gerling, M.-E. Pistol, L. Samuelson, W. Seifert, J.-O. Fornell, and L.-Å. Ledebo, Appl. Phys. Lett. **59**, 806 (1991).
[20]G. Bastard, Phys. Rev. B **24**, 5693 (1981).
[21]W. Seifert, J.-O. Fornell, L.-Å. Ledebo, M.-E. Pistol, and L. Samuelson, Appl. Phys. Lett. **56**, 1128 (1990).
[22]D. E. Aspnes, Surf. Sci. **37**, 418 (1973).
[23]P. C. Klipstein and N. Apsley, J. Phys. C **19**, 6461 (1986).
[24]D. Huang, D. Mui, and H. Morkoç, J. Appl. Phys. **66**, 358 (1989).
[25]B. Jusserand and M. Cardona, in *Light Scattering in Solids V,* edited by M. Cardona and G. Güntherodt (Springer-Verlag, Berlin, 1989).
[26]R. London, Adv. Phys. **13**, 423 (1964).
[27]F. Cerdeira, C. J. Buchenauer, F. H. Pollak, and M. Cardona, Phys. Rev. B **5**, 580 (1972).
[28]P. Wickboldt, W. Anastassakis, R. Sauer, and M. Cardona, Phys. Rev. B **35**, 1362 (1988).